

HRMA Tilts at XRCF

William Podgorski

In this section we discuss HRMA rigid body misalignments (relative P-H tilt and decenter). Data is presented from the optical alignments at Kodak, from the XRCF calibration and from various analyses.

Relative rigid body misalignments of the P to H optics in either decenter or tilt cause a comatic image distortion in the focal plane. This distortion is a “coma circle” in which the position of the rays in the coma circle moves around the circle twice as the input ray bundle (to the shell) varies once around the shell input aperture. Figure 28.1 illustrates this. The coma circle diameter in the focal plane is related to the P-H decenter and tilt angle as follows:

	1" P-H tilt	1 mm P-H decenter
Coma circle radius (")	1	10
Coma circle radius (μm)	48.5	488

28.1 Coordinate Systems and tilt angles

Since tilt and decenter both produce coma in the image plane we will interpret this coma as a tilt of the H optic relative to the P optic. Three different coordinate systems and sets of tilt angles have been used (see also Chapter B and Figure B.1):

- HRMA Coordinates (θ_Y, θ_Z)
- SAOSac Raytrace Coordinates ($azmis, elmis$)
- XRCF Coordinates ($tilt_Y, tilt_Z$)

The tilt angles are interpreted as a rotation of the H optic about a given coordinate axis, relative to the perfectly aligned P optic. The rotation axes are as follows (again see Figure B.1);

Coordinates	H Angle	Rotation axis
HRMA	θ_Y	+Y-HRMA
	θ_Z	+Z-HRMA
SAOSAC	$azmis$	+Y-OSAC
	$elmis$	-X-OSAC
XRCF	$tilt_Y$	+Y-XRCF
	$tilt_Z$	+Z-XRCF

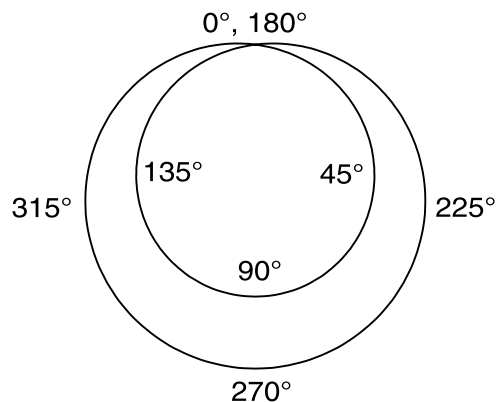


Figure 28.1: Schematic of coma circle (2θ) image distortion. The limaçon is the pattern of the photons at the focal surface. The angles refer to the azimuth of the optic at which the photons were reflected.

Tilt angle relationships:

$$\begin{aligned} azmis &= -\theta_Z = +tilt_Z \\ elmis &= -\theta_Y = +tilt_Y \end{aligned}$$

Table 28.1 provides a summary of relative tilt angles (H with respect to P) for various conditions. The four HRMA shells are given with the two tilt angles per shell. These angles are shown in terms of the XRCF angles, $tilt_Y$ and $tilt_Z$. The tilt angles as measured at Kodak by the HATS (in the final ATP measurements) are shown in line 1. In lines 2 and 3 the XRCF 1G *corrections* to the tilt angles are given for both SAO's FEA model and EKC's FEA model. Note that the corrections are about XRCF Y only, Y being the horizontal axis at XRCF. Lines 4 through 9 present various raytrace predictions of the tilt angles, based on various HRMA models and using a simulated quad shutter tilt calculation. The cases are defined as follows:

EKCHDOS04 Based on Kodak test data of 9/96 with *no* decenter, full XRCF mirror maps (SAO)

EKCHDOS04_low Based on Kodak test data of 9/96 with *no* decenter, mirror map includes only 3 term Legendre fit of surface (no 1G)

EKCHDOS04_low_off Based on Kodak test data of 9/96 with *no* decenter, mirror map includes only 3 term Legendre fit of surface (no 1G), HRMA pointed 1' off-axis in azimuth

EKCHDOS05 Based on Kodak ATP test data of 11/96 with XRCF measured decenter, full XRCF mirror maps (SAO), axial spacing as in EKCHDOS04

EKCHDOS05_low Based on Kodak ATP test data of 11/96 with XRCF measured decenter, mirror map includes only 3 term Legendre fit of surface (no 1G)

EKCHDOS06 Based on Kodak ATP test data of 11/96 with XRCF measured decenter, full XRCF mirror maps (SAO), axial spacing derived from XRCF measurements

EKCHDOS06_off Based on Kodak ATP test data of 11/96 with XRCF measured decenter, full XRCF mirror maps (SAO), axial spacing derived from XRCF measurements, HRMA pointed 1' off-axis in azimuth

Table 28.1: HRMA Tilt Angles

	Model	Shell 1		Shell 3		Shell 4		Shell 6	
		Y ["]]	Z ["]]						
1	Kodak ATP HATS	0.03	-0.09	-0.02	0.07	0.00	0.06	-0.03	0.32
2	XRCF 1G Corr(SAO)	-0.24	0.00	-0.08	0.00	-0.12	0.00	-0.12	0.00
3	XRCF 1G Corr(EKC)	-0.23	0.00	-0.18	0.00	-0.21	0.00	-0.33	0.00
4	EKCHDOS04	-0.19	-0.15	-0.08	0.03	-0.13	0.07	-0.29	0.27
5	EKCHDOS04_low	0.04	-0.11	-0.03	0.06	0.00	0.05	-0.09	0.27
6	EKCHDOS04_low_off	0.04	0.04	-0.03	0.23	0.00	0.23	-0.09	0.47
7	EKCHDOS05	-0.01	-0.03	0.13	0.11	0.05	0.15	-0.05	0.38
8	EKCHDOS05_low	0.20	0.00	0.18	0.14	0.17	0.13	0.15	0.39
9	EKCHDOS06	-0.01	-0.03	0.13	0.11	0.04	0.15	-0.05	0.38
10	EKCHDOS06_off	-0.01	0.12	0.12	0.29	0.05	0.34	-0.05	0.58
11	Measured 1/5-6/97 [†]	-0.15	-0.14	-0.05	-0.06	-0.04	-0.08	-0.44	0.18
12	Measured 1/5-6/97	-0.17	-0.14	-0.07	-0.05	-0.05	-0.07		
13	Measured 2/7-8/97	-0.14	-0.02	-0.05	0.12	-0.04	0.04	-0.43	0.36
14	Kodak ATP+SAO XRCF	-0.21	-0.09	-0.10	0.07	-0.12	0.06	-0.15	0.32
15	Kodak ATP+EKC XRCF	-0.20	-0.09	-0.20	0.07	-0.12	0.06	-0.36	0.32

[†]XRCF tilts measured 1' off-axis in azimuth

Lines 11, 12 and 13 give the measured XRCF tilt angles for 3 different cases, using the quad shutter calculations. Lines 11 and 12 present data from tests on 1/5/97 and 1/6/97, when the HRMA was 1' off-axis in azimuth. The data in line 11 is the initial baseline tilt data from these tests. The data in line 12 is repeatability data in which the *top* quadrant was re-measured and used in conjunction with the initial data from the other three quadrants. The data in lines 11 and 12 should be the same. The data in line 13 is from the last series of focus/tilt measurements in Phase 1 (at Al K α), taken on 2/7/97 and 2/8/97. An important difference between this data and the data taken in early January is that the HRMA was on-axis for the February data, but was +1' off-axis in azimuth when the January data was taken.

Lines 14 and 15 give the arithmetic sums of the Kodak ATP tilt angles plus the XRCF 1G tilts for the SAO model (line 14) and the EKC model (line 15).

28.2 Tilt Measurements

Examination of the measured tilt data in Table 28.1 (lines 11 - 13) shows excellent agreement for all of the *tilt_Y* measurements, with a span of only 0.03" over all shells for the three sets of data. There are larger differences between the January and February data in *tilt_Z*, however. The February data show, for all four shells, numerically larger values of *tilt_Z*, the differences ranging from about 0.10" to 0.20". This discrepancy is due to the difference in HRMA alignment, specifically the 1' azimuth off-axis angle. Simulations show the same trend in tilt angles as the HRMA azimuth is varied. Comparison of raytrace cases EKCHDOS04_low *vs.* EKCHDOS04_low_off and EKCHDOS06 *vs.* EKCHDOS06_off show that the *tilt_Z* angles do increase as the HRMA azimuth is increased, by about the same amounts as seen in the measurements. In Table 28.2 the 1/5-6/97 data has been adjusted for the off-axis azimuth effect, line B, and compared with the 2/7-8/97 data, line C. The agreement is excellent, and we will therefore use the tilt values measured in 2/97 as our reference measurement, with the HRMA at an on-axis condition.

Table 28.2: Summary of HRMA Tilt Angles

	Model	Shell 1		Shell 3		Shell 4		Shell 6	
		Y ["]]	Z ["]]						
A	Offaxis Az delta	0.00	0.15	-0.01	0.18	0.01	0.19	0.00	0.20
B	1/5-6/97 + Az delta	-0.15	0.01	-0.05	0.12	-0.04	0.11	-0.44	0.38
C	Measured 2/7-8/97	-0.14	-0.02	-0.05	0.12	-0.04	0.04	-0.43	0.36
D	EKCHDOS06	-0.01	-0.03	0.13	0.11	0.04	0.15	-0.05	0.38
E	(Data - Model)	-0.13	0.01	-0.18	0.01	-0.08	-0.11	-0.38	-0.02

28.3 Comparison with models

The raytrace simulation denoted as EKCHDOS06 represents our best model of the HRMA at the XRCF to date. Calculations of tilt angles were made from it using the `wedge` program to simulate the quadrant shutters, in conjunction with the HXDS shutter focus algorithm. A comparison of the modeled tilts with measured tilts may be seen by comparison of lines C and D in Table 28.2. The differences in modeled vs. measured tilts are given in line E of Table 28.2. The differences in $tilt_Z$ are smaller than in $tilt_Y$. These differences may indicate a lack of accuracy in the XRCF 1G modeling of rigid body tilts, since only $tilt_Y$ is affected by gravity in XRCF testing, and it has the larger differences.

28.4 Future work

We plan to investigate the 1G models of the HRMA with respect to tilt to try to determine if there are modeling issues which may affect the tilts. If not, then we will “tune” the 1G models to the XRCF measured data, so that the modeled tilts are close to the measured tilts. This procedure is based on the assumption that the tilt data from the Kodak HATS tests is correct, as well as the XRCF data, and that the most likely source of error is the 1G model. This conclusion is supported by the agreement seen in the $tilt_Z$ values, which are not affected by gravity. One important result which follows from this assumption is that shell 6 will have significantly better performance on-orbit than at XRCF, since a large fraction of the $tilt_Y$ seen at XRCF is gravity induced. This assumption will be checked by examination of on-orbit image properties at high energies.

28.5 Quad shutter tilt data from XRCF tests

28.5.1 Shell 1

Runid	Date	TRW ID	Shell / Quad	Center [μm]	
				Y	Z
107656	01/06/97	D-IXF-P2-67.016	1T	-307159.66	10676.87
107657	01/06/97	D-IXF-P2-67.017	1N	-307147.69	10683.71
107659	01/06/97	D-IXF-P2-67.018	1B	-307152.50	10665.15
107660	01/06/97	D-IXF-P2-67.019	1S	-307146.31	10677.72

Y Tilt = -0.153014

Z Tilt = -0.143143

107663	01/06/97	D-IXF-P2-67.020	1T	-307159.59	10674.64
107657	01/06/97	D-IXF-P2-67.017	1N	-307147.69	10683.71
107659	01/06/97	D-IXF-P2-67.018	1B	-307152.50	10665.15
107660	01/06/97	D-IXF-P2-67.019	1S	-307146.31	10677.72

Y Tilt = -0.170591

Z Tilt = -0.143143

111470	02/07/97	E-IXF-P2-67.016	1T	-307110.59	10624.46
111471	02/07/97	E-IXF-P2-67.017	1N	-307102.25	10630.90
111474	02/07/97	E-IXF-P2-67.018	1B	-307109.31	10622.07
111475	02/07/97	E-IXF-P2-67.019	1S	-307115.00	10633.48

Y Tilt = -0.140715

Z Tilt = -0.0209302

28.5.2 Shell 3

Runid	Date	TRW ID	Shell / Quad	Center [μm]	
				Y	Z
107637	01/05/97	D-IXF-P2-67.001	3T	-307167.59	10676.34
107638	01/05/97	D-IXF-P2-67.002	3N	-307156.75	10688.66
107639	01/05/97	D-IXF-P2-67.003	3B	-307150.00	10680.82
107640	01/05/97	D-IXF-P2-67.004	3S	-307153.22	10674.62

Y Tilt = -0.0482356

Z Tilt = -0.0603847

107641	01/05/97	D-IXF-P2-67.005	3T	-307166.53	10674.11
107638	01/05/97	D-IXF-P2-67.002	3N	-307156.75	10688.66
107639	01/05/97	D-IXF-P2-67.003	3B	-307150.00	10680.82
107640	01/05/97	D-IXF-P2-67.004	3S	-307153.22	10674.62

Y Tilt = -0.0658127

Z Tilt = -0.0517239

111451	02/07/97	E-IXF-P2-67.001	3T	-307116.59	10613.04
111452	02/07/97	E-IXF-P2-67.002	3N	-307110.19	10634.03
111453	02/07/97	E-IXF-P2-67.003	3B	-307112.28	10644.09
111454+7 [†]	02/07/97	E-IXF-P2-67.004	3S	-307134.19	10629.06

[†]This run included an extra 1D scan

Y Tilt = -0.0469876

Z Tilt = 0.122213

28.5.3 Shell 4

Runid	Date	TRW ID	Shell / Quad	Center [μm]	
				Y	Z
107642	01/05/97	D-IXF-P2-67.006	4T	-307163.59	10677.85
107644	01/05/97	D-IXF-P2-67.007	4N	-307153.69	10685.39
107645	01/05/97	D-IXF-P2-67.008	4B	-307152.19	10679.59
107646	01/05/97	D-IXF-P2-67.009	4S	-307151.97	10677.10

Y Tilt = -0.0397929

Z Tilt = -0.0798714

107647	01/05/97	D-IXF-P2-67.010	4T	-307162.38	10676.75
107644	01/05/97	D-IXF-P2-67.007	4N	-307153.69	10685.39
107645	01/05/97	D-IXF-P2-67.008	4B	-307152.19	10679.59
107646	01/05/97	D-IXF-P2-67.009	4S	-307151.97	10677.10

Y Tilt = -0.0484686

Z Tilt = -0.0702483

111458	02/07/97	E-IXF-P2-67.006	4T	-307114.69	10629.45
111459	02/07/97	E-IXF-P2-67.007	4N	-307119.09	10630.60
111460	02/07/97	E-IXF-P2-67.008	4B	-307119.66	10630.07
111461	02/07/97	E-IXF-P2-67.009	4S	-307119.84	10634.37

Y Tilt = -0.0429504

Z Tilt = 0.0358459

28.5.4 Shell 6

Runid	Date	TRW ID	Shell / Quad	Center [μm]	
				Y	Z
107655	01/05/97	D-IXF-P2-67.015	6T	-307157.16	10641.41
107652	01/05/97	D-IXF-P2-67.012	6N	-307162.00	10681.58
107653	01/06/97	D-IXF-P2-67.013	6B	-307143.06	10654.70
107654	01/06/97	D-IXF-P2-67.014	6S	-307161.69	10669.99

Y Tilt = -0.43721

Z Tilt = 0.184763

111462	02/07/97	E-IXF-P2-67.011	6T	-307109.50	10600.10
111463	02/07/97	E-IXF-P2-67.012	6N	-307136.59	10626.19
111466	02/07/97	E-IXF-P2-67.013	6B	-307113.44	10599.34
111467	02/07/97	E-IXF-P2-67.014	6S	-307131.88	10628.12

Y Tilt = -0.432541

Z Tilt = 0.359181